Effect of Slope Shape on Side Slope Stability under Seismic Action

Hang Chen[1,2], Xuemei Long[2], Xi Huang[1], Zuyin Zou[2],Qixiang Yan[1,*]

[1] College of Civil Engineering, Southwest Jiaotong University, Chengdu, China, 610031

[2] College of Civil Engineering, Sichuan Agricultural University, Dujiangyan, China,611830

**Corresponding author; e-mail: chenhangssd@163.com*

ABSTRACT

In order to study the effect of different slope shapes on side slope stability under seismic action, models of side slopes with multiple shapes, i.e., different declivities, concavities, convexities and steps, etc. are built, using FLAC3D finite difference software. Wenchuan Earthquake stress time history is applied, to compare stress-strain relationship and stability of side slopes with different shapes under seismic action. The results show that free slope surfaces have an amplification effect on the input seismic waves. The horizontal displacement and acceleration of slope surfaces increase with height and declivity. With the increase of slope concavity, shear stress increment is concentrated on the slope shoulder. The slope shoulder becomes increasingly unstable. With the increase of slope convexity, shear stress increment is concentrated on the slope waist. The slope waist becomes increasingly unstable. Steps may weaken the acceleration amplification effect of slope surface. The more steps, the more stable.

KEYWORDS: Slope; Stability; Earthquake; Slope shapes

INTRODUCTION

China is located on the southeast edge of the Eurasian plate and adjoins the Pacific plate and the Indian Ocean plate. The geological environment is complex. All kinds of geological disasters occur frequently. As a seismically active country, the occurrence of earthquakes in China has caused a large number of casualties and property losses and led to numerous secondary geological disasters. Historical data show that M_S8.0 Wenchuan Earthquake on May 12, 2008 triggered over 197,000 landslides[1]. Related studies show that the formation and development of landslides are affected by many factors, such as climate, topography, regional geology and social economy, etc[2]. At the same time, internal factors of side slopes, including micro topography (declivity, concavity/convexity and steps, etc.) and slope structure, plays a controlling role in forming landslides[3]- [6]. At present, many scholars have carried out lots of research on the effect of earthquakes on side slopes: Wang Duojun et al. [7] studied the slope surface effect of bedding rock slopes under seismic action, using UDEC software. Yan Zhixin et al. [8] discussed the stability of three shapes of rock slopes under seismic action, based on FLAC3D software. He Liu et al. [9] conducted a model-based experimental study of the instability and failure of soil slopes with different shapes, using a self-made one-way vibrostand. Yang Guoxiang et al. [10] adopted a large indoor vibrostand model test, with large rock side slopes triggered by Wenchuan Earthquake as the research object. By entering different frequencies, durations and amplitudes of sine waves, they explored the effect of acceleration response characteristics and dynamic input parameters of bedding and homogeneous rock side slopes on

dynamic characteristics of side slopes. However, at present there are rare studies on the effect of slope shape on side slope stability under seismic action.

Drawing on previous studies, this article makes an analysis of the stability of a total of 3 groups and 11 side slopes with different declivities, concavities, convexities and steps under seismic action, based on finite difference software FLAC3D, to probe into the effect law of slope shape on side slope stability and their relationship, provide basic data for the study of slope stability under seismic action and offer technical basis to the prevention and control of similar slopes.

THEORETICAL BASIS OF NUMERICAL SIMULATION

The basic principle of FLAC3D is the Lagrangian difference method. This method solves kinematic equation and dynamic equation based on explicit difference method, using lumped mass of grid nodes obtained from true density in the surrounding area. It can not only simulate certain duration of earthquake process, but also eliminate reflection of seismic waves on boundaries using viscous boundary. Using Mohr-Coulomb model, the program calculates permanent deformation automatically and also simulates the effect of propagation of compression waves and shear waves and their coupling on materials. It has its unique features in the dynamic analysis of side slopes.

Load Conversion

This article adopts Wenchuan Earthquake acceleration time history. After corrected with baseline, velocity time history is obtained by integration. Finally, stress time history is obtained through Eq.(1) and input from the bottom of model.

$$\begin{cases} \sigma_s = 2(\rho C_s)V_s \\ \sigma_n = 2(\rho C_\rho)V_n \end{cases} \tag{1}$$

where C_s、C_ρ are given by Eq.(2).

$$\begin{cases} C_s = \sqrt{\dfrac{G}{\rho}} \\ C_\rho = \sqrt{\dfrac{K + \dfrac{4G}{3}}{\rho}} \end{cases} \tag{2}$$

where σ_s is tangential stress, σ_n is normal stress, ρ is material density, C_s is velocity of S wave, C_ρ is velocity of P wave, V_s is tangential velocity at a given point, V_n is normal velocity at a given point, G is shear modulus of materials and K is bulk modulus of materials.

Selection of Damping

The mass component in Rayleigh damping is equivalent to a damper that connects each node and ground and stiffness component is equivalent to a damper that connects units. By choosing an appropriate coefficient, a response irrelevant to frequency can be obtained approximately within a limited frequency range. The damping matrix C and stiffness matrix K in dynamic equation is related to mass matrix K. The minimum critical damping ratio $\xi_{\min}$ and minimum center frequency $\omega_{\min}$ of

Rayleigh damping can be determined by estimating the minimum of damping ratio curve of superposition results:

$$C = \alpha M + \beta K \quad (3)$$

$$\xi_{\min} = (\alpha \bullet \beta)^{\frac{1}{2}} \quad (4)$$

$$\xi_{\min} = (\alpha / \beta)^{\frac{1}{2}} \quad (5)$$

where α is damping constant in proportion to mass. β is damping constant in proportion to stiffness

SELECTION OF SLOPE SHAPE

Side slopes have complex and varied shapes. Side slopes formed by both natural weathering and seismic action can be divided into four basic types, i.e., convex, concave, straight and step or their combinations. To study the effect of different slope shapes on side slope stability under seismic action, the following three aspects are selected to make a simplified comparative analysis:

(1) The effect of declivity on side slope stability on straight slope;

(2) The effect of convexity and concavity on side slope stability on straight, convex and concavity slopes;

(3) The effect of steps of side slope stability on step slope.

ESTABLISHMENT OF NUMERICAL MODEL

Model Size and Monitoring Site Arrangement

The basic model size is 300m long, 70m wide and 150m tall. For ease of comparative analysis, models of side slopes of different shapes are grouped as follows:

(1) Declivity Group

3 models of different declivities are set up. The declivities are 1:1.6, 1:1.3 and 1:1 respectively. Monitoring sites, i.e., Slope Shoulder A, Slope Waist B and Slope Toe C are arranged on the slope surface of 3 models of different declivities, as shown in Fig.1.

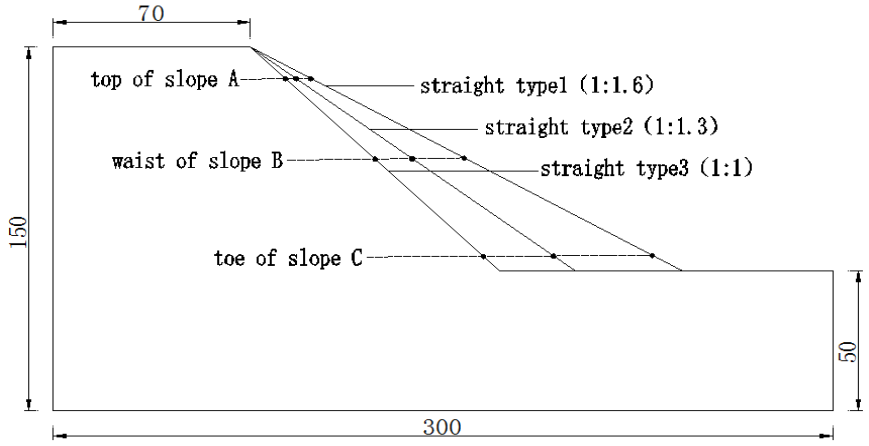

Figure 1: The effect of declivity on model size and monitoring site

(2) Concavity and Convexity Group

5 models of different concavities and convexities are set up, including 2 concave types, 1 straight type and 2 convex types respectively. Monitoring sites, i.e., Slope Shoulder A, Slope Waist B and Slope Toe C are arranged on the slope surface of 5 models of different concavities and convexities, as shown in Fig.2.

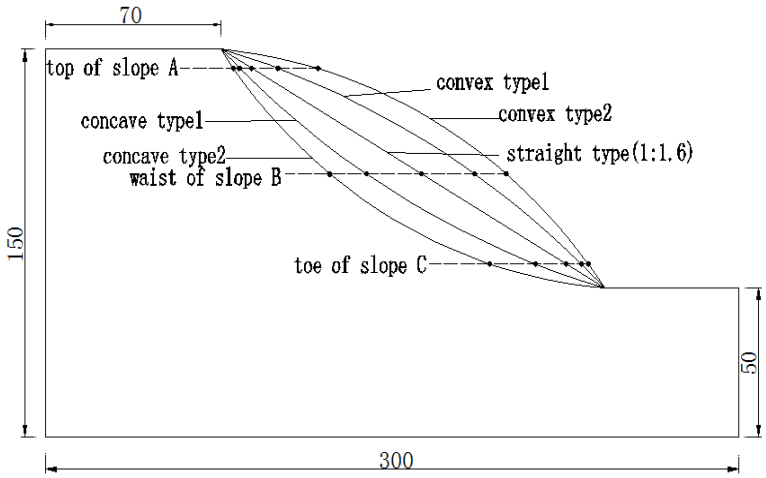

Figure 2: The effect of declivity on modelsize and monitoring site

(3) Step Group

3 models of different steps are set up, including straight type, one step type and two steps type respectively. Slope Shoulder A_1, Slope Waist B_1 and Slope Toe C_1 are arranged on the slope surface of stepless model. Slope Shoulder A_2, Slope Waist B_2 and Slope Toe C_2 are arranged on the slope surface of one step model. Slope Shoulder A_3, Slope Waist B_3 and Slope Toe C_3 are arranged on the slope surface of two steps model, as shown in Fig.3.

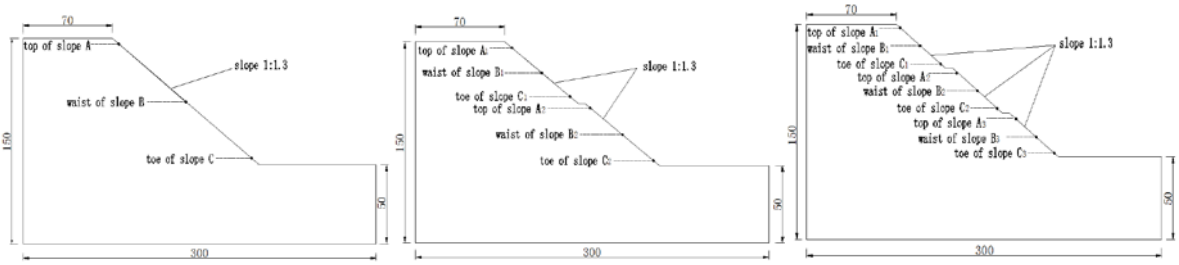

(a) straight type (b)one step type (c)two steps type

Figure 3: The effect of slope steps on model size and monitoring site

Model Materials

The present study focuses on exploring the effect of slope shape on side slope deformation under seismic action. So the effect rainfall, human activities and other external factors on this model is not taken into consideration. Suppose that the side slope is a homogeneous one. Using Mohr-Coulomb model, converting with the following elastic-mechanical formula, the bulk modulus (*K*) and shear modulus (*G*) of materials and physical and mechanical parameters of side slopes are obtained, as shown in Tab. 1.

$$K = \frac{E}{3(1-2\upsilon)} \quad (6)$$

$$G = \frac{E}{2(1+\upsilon)} \quad (7)$$

where K is bulk modulus, G is shear modulus, E is elastic modulus and υ is Poisson's ratio.

Table.1 Physical and mechanical parameters of gravel-soil

	bulk density	cohesion	friction angle	elastic modulus	Poisson's ratio	tensile strength
Unit	D/kg.m^3	C/KPa	Φ/°	E/MPa	V	σ_t/MPa
Silt Clay	2150	22	17	41	0.35	0

Boundary Conditions and Damping Setting of the Models

Free field boundaries are set around models. Group assignment is conducted on the generated free field grids, to ensure that the propagation characteristics on artificial boundaries are the same as those in original continuous medium. FLAC3D contains Rayleigh damping, local damping and hysteretic damping. Considering that the theory of Rayleigh damping is similar to conventional dynamic analytical method and that practice has proved that acceleration response rules derived from Rayleigh damping are more consistent with reality, this article uses Rayleigh damping and defines the minimum critical damping ratio as 5% and the minimum center frequency as 16.8.

Selection and Conversion of Seismic Waves

SV waves in Wenchuan Earthquake waves are selected. Fig. 4 shows Wenchuan Earthquake acceleration time history. The peak acceleration is 0.3g. The duration is 20s. The equivalent load of Wenchuan Earthquake waves is calculated with mathematical software MATLAB, compiled into a table file and input into FLAC3D to realize the function of seismic waves.

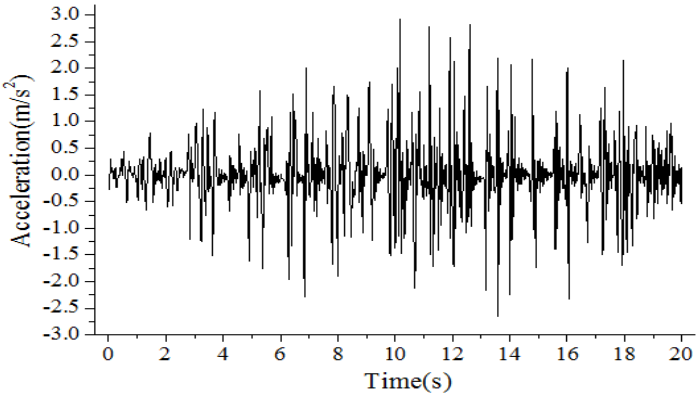

Figure 4: Wenchuan earthquake acceleration time history

CALCULATION OF EACH GROUP OF MODELS AND RESULT ANALYSIS

Declivity Group

The acceleration, speed and displacement of monitoring sites along the slope surface of side slopes with 3 different declivities are calculated and recorded. To describe corresponding rules of side slope surface acceleration under dynamic seismic action, the ratio between the peak acceleration in each monitoring site on the slope surface and the peak acceleration of seismic wave input from the bottom of model is defined as PGA amplification coefficient. According to data in each monitoring site, PGA amplification coefficient in each monitoring site on slopes with different declivities (see Fig. 5) and the horizontal displacement of each monitoring site (see Fig.6) are obtained after treatment.

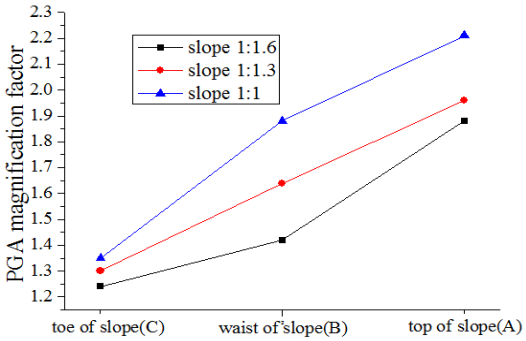

Figure 5: The horizontal PGA amplification coefficient of each monitoring site

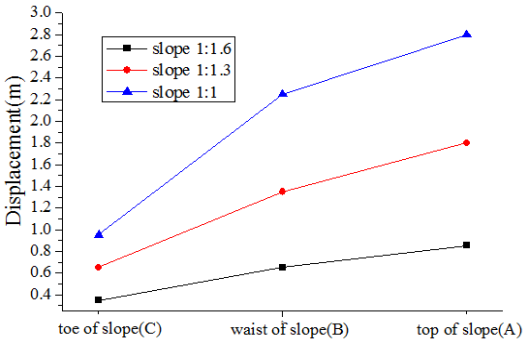

Figure 6: The horizontal displacement of each monitoring site

From Fig. 5, PGA amplification coefficient tends to increase with height. Comparing PGA amplification coefficients of each monitoring site in the horizontal direction on slope surfaces with different declivities, we can know that PGA amplification coefficient tends to increase with declivity. From Fig. 6, each monitoring site on the slope surface of 3 side slopes has a different size of horizontal displacement. The overall horizontal displacement of side slope with a declivity of 1:1.6 is between 0.35m and 0.85m. The overall horizontal displacement of side slope with a declivity of 1:1.3 is between 0.65m and 1.85m. The overall horizontal displacement of side slope with a declivity of 1:1 is between 0.95m and 2.85m. This indicates that none of the slopes are stable under seismic action, but the instability of different slopes with declivities varies. The side slope with a declivity of 1:1.6 is relatively stable. The side slope with a declivity of 1:1.3 has local slides, but not destroyed as a whole. The side slope with a declivity of 1:1.3 has a wide range of slides. The side slope is destroyed as a whole. From the size of horizontal displacement at each monitoring site on each slope, it can be concluded that horizontal displacement of slope surface increases with height and declivity. This is consistent with the PGA amplification coefficient of slope surface.

Concavity and Convexity Group

The acceleration, speed and displacement of monitoring sites along the slope surface of side slopes with 5 different concavities and convexities are calculated and recorded. The cloud chart of residual shear strain increment of each side slope is drawn and shown in Fig. 7 and 8. (Concavity: Concave Type 2 > Concave Type 1; convexity: Convex Type 2 > Convex Type 1)

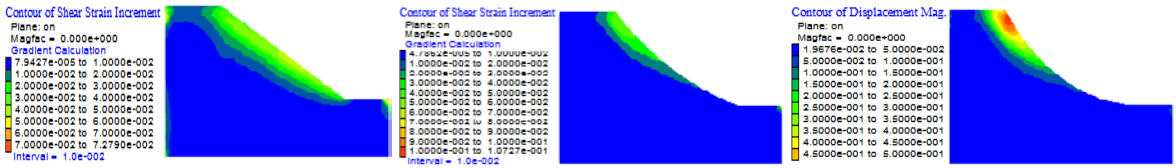

(a)straight type (b)concave type 1 (c)concave type 2

Figure 7: The shear strain increment cloud of slope with different concavity

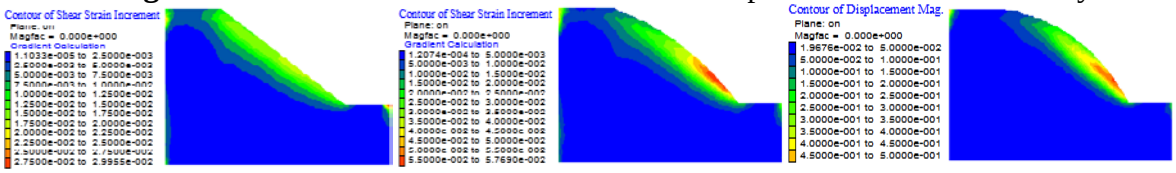

(a)straight type (b)convex type1 (c)convex type2

Figure 8: The shear strain increment cloud of slope with different convexity

From Fig.7, residual shear strain increment increases with the concavity of side slope. The maximum residual shear strain increments of straight type, Concave Type 1 and Concave Type 2 were 0.07, 0.11 and 0.5 respectively. The approximate uniform distribution of straight type gradually moves upwards along slope surface to concentrated distribution in the slope shoulder. It can be inferred that the horizontal displacement of concavity slope is mainly concentrated in slope shoulder. From Fig.8, shear strain increment increases with the convexity of side slope. The maximum residual shear strain increments of straight type, Convex Type 1 and Convex Type 2 were 0.03, 0.07 and 0.5 respectively. The approximate uniform distribution of straight type gradually moves downwards in the center along slope surface to concentrated distribution in the slope waist. It can be inferred that the horizontal displacement of convexity slope is mainly concentrated in slope waist. In addition, the failure modes of concavity and convexity slopes are different.

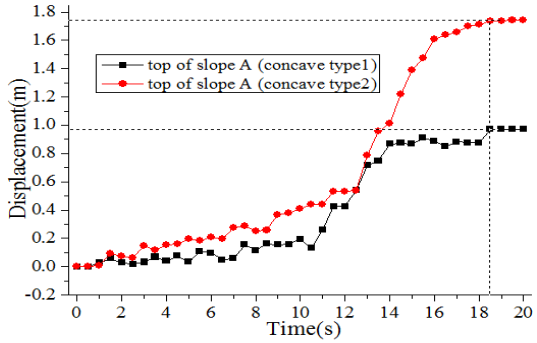

Figure 9: The horizontal displacement of point A on concavity slope shoulder

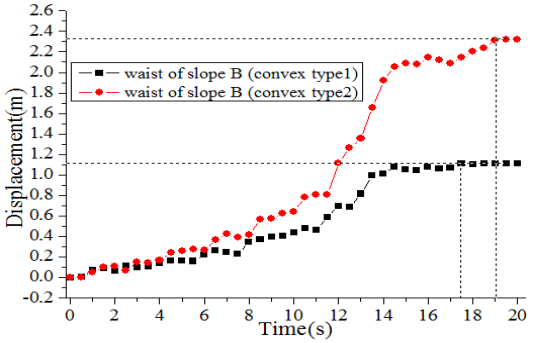

Figure 10: The horizontal displacement of point B on slope waist

Fig.9 shows the horizontal displacement of Point A on concavity slope shoulder. Comparing the horizontal displacements of Concave Type 1 and Concave Type 2 slope shoulders, we can know that the final horizontal displacement of Concave Type 2 is 1.75m, greater than that of Concave Type 1, 0.98m. Fig.10 shows the horizontal displacement of Point B on convexity slope waist. Comparing the horizontal displacements of Convex Type 1 and Convex Type 2 slope waists, we can know that the final horizontal displacement of Convex Type 2 is 2.33m, greater than that of Convex Type 1, 1.11m. Analysis shows when a side slope is convex, potential slide surface lies in slope shoulder. The greater concavity, the greater horizontal displacement of slope shoulder, the more unstable the side slope is. When a side slope is concave, potential slide surface lies in slope waist. The greater convexity, the greater horizontal displacement of slope waist, the more unstable the side slope is.

Step Group

The acceleration, speed and displacement of monitoring sites along the slope surface of side slopes with 3 different steps are calculated and recorded. The horizontal displacement of each monitoring site with time is shown in Fig. 11.

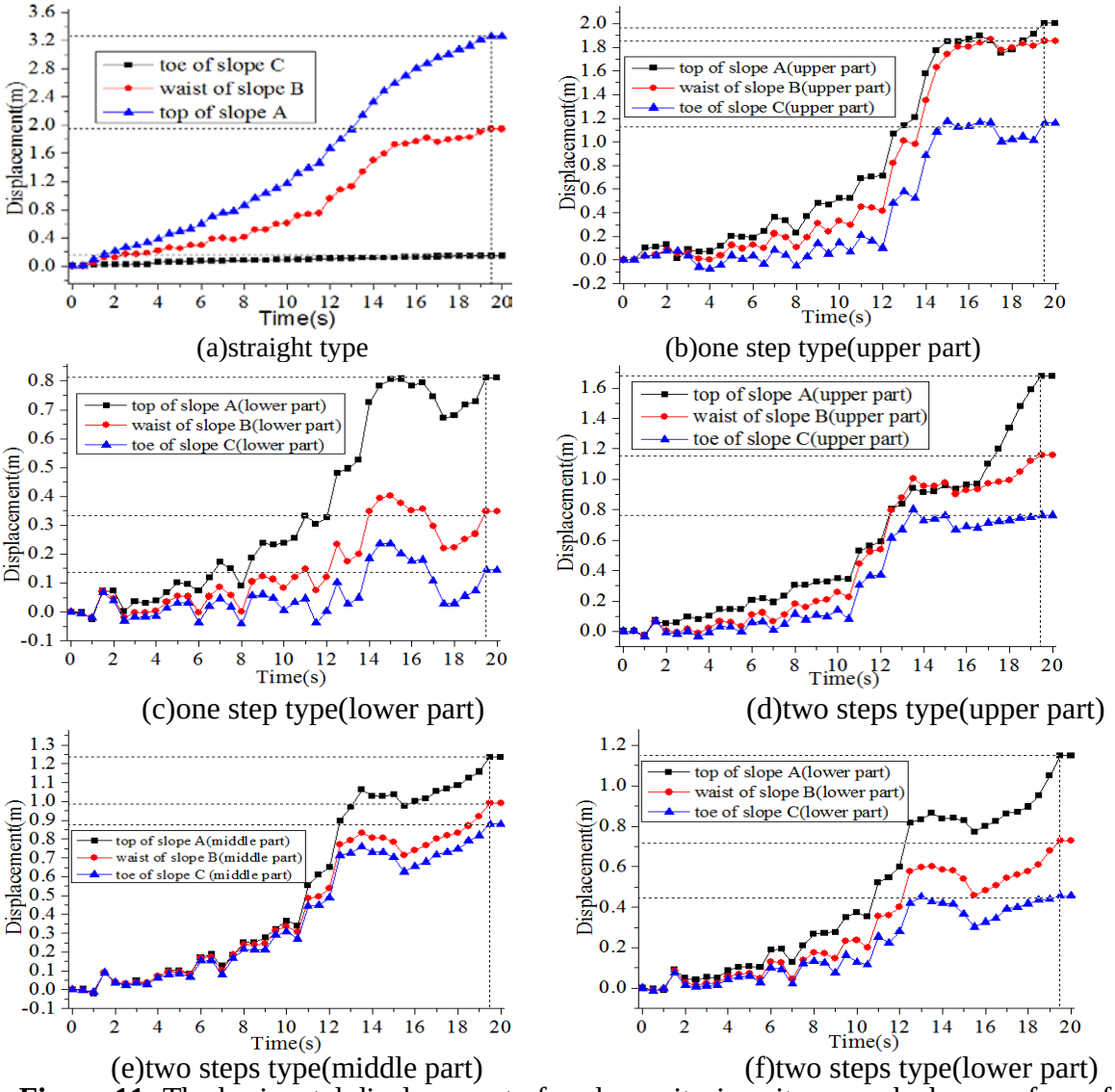

Figure 11: The horizontal displacement of each monitoring site on each slope surface of step type slope

From Fig. 11, the change rules of the horizontal displacement in each slope section divided by steps and the horizontal displacement of the entire slope are roughly the same. Their values increase with height along the slope surface. For 3 side slopes with the same declivity and overall height but different steps, their respective overall horizontal displacements differ. The overall horizontal displacement of stepless slope is the largest, between 0.27m and 3.25m, followed by that of one step slope, between 0.15m and 1.98m. The overall horizontal displacement of two steps slope is the smallest, between 0.44m and 1.68m. This suggest that for side slopes with the same declivity and height, under seismic action, the more steps there are on the slope surface, the more stable side slopes are. Analysis shows that when seismic waves are propagating along the slope surface, steps may

weaken the amplification effect of peak acceleration on the side slope surface and reduce displacement. Meanwhile, steps divide a long and high slope into several small surfaces, reduce the height of slope surface, weaken the amplification effect of peak acceleration on slope surface and further reduce displacement.

CONCLUSIONS

This paper carries out a dynamic response simulation experiment of side slopes with different concavities, convexities and steps under seismic action, using finite difference software FLAC3D. Through a lot of numerical calculation and comparisons between different models, we gain the following insights into side slopes under seismic action:

(1) The deformation and failure sites of slopes with different shapes under seismic action differ from each other. The deformation and failure of slopes under seismic action is closely related to the slope shape.

(2) Under seismic action, the concavity and convexity of slope surface has a distinct effect on the position of potential slide surface on the side slope. With the increase of slope concavity, shear stress increment is concentrated on the slope shoulder. The slope shoulder becomes increasingly unstable. With the increase of slope convexity, shear stress increment is concentrated on the slope waist. The slope waist becomes increasingly unstable. Steps may weaken the amplification effect of slope surface acceleration. The more steps, the more stable.

(3) Suggestions on the prevention and treatment of side slopes: to reduce the declivity of slope surface, reinforce the slope shoulder of concavity slopes, reinforce the lower central waist of convexity slopes, set up multiple steps for high side slopes to increase stability, while strengthening the reinforcement of shoulder and lower central waist.

ACKNOWLEDGEMENTS

The research is supported by supported by the Innovation Training Project of Sichuan Agricultural University under NO. 040606693 and NO.1510626105.

REFERENCES

1. Chong Xu, Xi-wei Xu, Xi-yan Wu,(2013)"Detailed catalog of landslides triggered by the 2008 WEN-CHUAN earthquake and statistical analyses of their spatial distribution, "*Journal of Engineering Geology* Vol.21,No.1,pp 25-44.
2. Li Jun-xia, Wang Chang-ming, Wang Gang-cheng,(2010)"Analysis of landslide influential factors and coupling intensity based on third theory of quantification, "*Chinese Journal of Rock Mechanics and Engineering(Natural Science)* Vol.29,No.6,pp 1206-1213.
3. Jiang-hong Chen, Liang-peng Wan, Hua-feng Deng, et al.(2016) "Factor Sensitivity Analysis of Three Gorges Reservoir Slope Stability," *Electronic Journal of Geotechnical Engineering* Vol.21,No.8,pp 1871-1884. Available at ejge.com.
4. Failab Benzenine, M. A. Allal,(2016) " Mapping of Hazard of Slope Movement Application for the Municipality o fBensekrane, Algeria," *Electronic Journal of Geotechnical Engineering* Vol.21,No.7,pp 1597-1609. Available at ejge.com.

5. Qi Fuqiang (2016) " Seismic Dynamic Response of Sandy Slope under the Coupling of Earthquake and Groundwater," *Electronic Journal of Geotechnical Engineering* Vol.21,No.7,pp 1733-1745. Available at ejge.com.
6. Jun-zhi Lin, Ze-long Liang (2016) "The Application of Extension Neural Network in the Stability Analysis of High Rock Slope," *Electronic Journal of Geotechnical Engineering* Vol.21,No.7,pp 1705-1716. Available at ejge.com.
7. Wang Duo-jun, Pei Xiang-jun, Song Jin-long (2012)"Topography effects on defomation and failuar of bedding rock slope under earthquake, "*highway* Vol.1,No.8,pp 12-16.
8. Yan Zhi-zhong, Shi Sheng, Li Bin (2013)"Influence of the slope shape on the stability of rock slope under seismic, "*Journal of Shandong University of Science and Technology,"(Natural Science)* Vol.32,No.2,pp 43-48.
9. He Liu, Wu Guang, Zhao Zhi-ming (2014)"Model test of influence of slope surface morphology on dynamic deformation failure, *"Rock and Soil Mechanics,"* Vol.33, No.1,pp 111-117.
10. Yang Guo-xiang, Wu Fa-quan, Dong Jin-yu (2012)"Study of dynamic response characters and failure mechanism of rock slope under earthquake, "*Journal of earthquake engineering and engineering vibration,"*Vol.31,No.4,pp 696-702.